The 1998 Oklahoma–Texas Drought: Mechanistic Experiments with NCEP Global and Regional Models

SONG-YOU HONG

Department of Atmospheric Sciences, Yonsei University, Seoul, Korea

EUGENIA KALNAY

Department of Meteorology, University of Maryland, College Park, College Park, Maryland

(Manuscript received 26 February 2001, in final form 25 July 2001)

ABSTRACT

This study presents results from mechanistic experiments to clarify the origin and maintenance of the Oklahoma–Texas (OK–TX) drought of the 1998 summer, using the National Centers for Environmental Prediction (NCEP) global and regional models. In association with this unprecedented drought, three major mechanisms that can produce extended atmospheric anomalies have been identified: (i) sea surface temperature (SST) anomalies, (ii) soil moisture anomalies, and (iii) atmospheric initial conditions favorable to such a climate extreme even in the absence of surface forcing (i.e., internal forcing).

The authors found that the SST anomalies during April–May 1998 established the large-scale conditions for the drought. However, the warm El Niño–Southern Oscillation (ENSO) SST anomalies over the central and eastern tropical Pacific alone did not play a major role in initiating the drought. The internal structure of atmospheric conditions played as significant a role as the SST anomalies over the globe. In June 1998, soil moisture anomalies started to play an important role in maintaining the drought, and the regional positive feedback associated with lower evaporation/lower precipitation explained most of the water deficit in July. After July, synoptic-scale disturbances overwhelmed the impact of dry soil moisture near the Gulf of Mexico states where above-normal precipitation occurred, but the regional feedback was still prominent over the OK–TX region, where the drought persisted until early October.

1. Introduction

Extreme dryness during April–June 1998 covered much of the south-central and southeastern United States, with record-low rainfall totals dating back to 1895 observed in New Mexico, Texas, Louisiana, and Florida. This unprecedented abnormal local climate was a serious problem, in particular, over the Oklahoma–Texas (OK–TX) region where the drought persisted until early fall of 1998. The Oklahoma mesonet showed that soil moisture reached levels comparable or lower to those of the 1930s Dust Bowl (Basara et al. 1999; Bell et al. 1999). By May, a circulation typical of midsummer had already been established, with high temperatures and low precipitation normally observed during July and August. This circulation persisted until early October throughout most of Oklahoma and Texas, except in some areas of southern Texas, where it rained in August and September.

Corresponding author address: Song-You Hong, Dept. of Atmospheric Sciences, College of Science, Yonsei University, 134 Sinchon-dong, Seoul, 120-749 Korea.
E-mail: shong@yonsei.ac.kr

There are three mechanisms that could be associated with extended atmospheric anomalies. The first two are associated with anomalous surface forcing: 1) sea surface temperature (SST) anomalies, and 2) soil moisture (SM) anomalies. The third mechanism is the presence of an atmospheric circulation at the beginning of a period leading to persistent anomalies even in the absence of surface forcing. In this paper we explore the role that each of these mechanisms had in the establishment and maintenance of the OK–TX drought.

Climatologically, summertime precipitation and temperature in the United States are significantly correlated with the SST anomalies in the Pacific such as those associated with El Niño and La Niña episodes (Ting and Wang 1997; Montroy 1997; Montroy et al. 1998). For the 1988 drought over the Great Plains, studies suggested that it was rooted in the cold SST anomalies in the tropical Pacific (Trenberth et al. 1988; Trenberth and Branstator 1992; Palmer and Brankovic 1989; Namias 1991; Lyon and Dole 1995; Chen and Newman 1998). Trenberth et al. (1988), Palmer and Brankovic (1989), and Namias (1991) proposed that the heat wave and drought in the United States during 1988 were primarily associated with a persistent anomalous upper-level cir-

culation pattern that linked to the SST anomalies in the *eastern* tropical Pacific, whereas Lyon and Dole (1995), and Chen and Newman (1998) argued that the SST anomalies in the eastern Pacific did not play a significant role in exciting a wave train associated with intense anticyclonic circulation. Rather, they suggested that remote forcing such as cold SST anomalies in the *western* Pacific played a predominant role in initiating the drought.

Whereas SST anomalies can force droughts through teleconnections, soil moisture tends to produce a local positive feedback. Dry (moist) soil reduces (increases) local evaporation and therefore can reduce (increase) regional precipitation (Shukla and Mintz 1982; Fennessy and Shukla 1999). Atlas et al. (1993) and Wolfson et al. (1987) examined the local feedback between soil moisture and precipitation with numerical experiments, for the 1988 and 1980 drought events, respectively. These studies stressed that anomalous soil moisture in North America played an important role in initiating and maintaining the drought over the Great Plains through a positive feedback between the atmosphere and the land. Koster et al. (2000) performed thousands of years of general circulation model simulations, which indicate that land surface initial conditions can have a large impact on the predictability over transition regions between wet and dry areas. In particular, they found that for the late spring and summer, there is a maximum in the ensemble-forecast coherence over the Gulf of Mexico states, extending to Oklahoma and farther north. They found that the impact of land surface anomalies on predictability over this region in late spring and summer is even larger than the overall impact of SST anomalies.

Since the 1997/98 winter underwent one of the strongest El Niño–Southern Oscillation (ENSO) episodes on record in the twentieth century (rivaling the 1982/83 event) that produced many major changes in the global circulation, it is natural to assume that the OK–TX drought could be ''blamed on El Niño.'' There are two problems, however, with this simple-minded approach. First, ENSO episodes tend to be somewhat correlated with high precipitation in April–June over OK–TX (Ting and Wang 1997; Montroy et al. 1998; Montroy 1997). Furthermore, as indicated above, numerical studies of the 1988 drought suggest that the cold SST anomalies in the tropical Pacific (La Niña) established the drought in the United States (Trenberth et al. 1988; Atlas et al. 1993; Chen and Newman 1998). Second, the warm ENSO episode faded in the late spring/early summer, and the drought persisted by early fall of 1998 in most of the OK–TX region. In a review of the 1998 climate, Bell et al. (1999) suggested that residual warm waters in the extreme eastern Pacific during the dissipation stage of the warm ENSO case maintained the amplified subtropical ridge over the southern United States and Mexico throughout the summer. Their scenario is based on the data analysis and does not explain the early development of the drought in April–May when the warm ENSO episode is strong. Compared to the 1988 drought in the Great Plains, the drought of 1998 is localized in the southern United States. Recognizing these unique features of the 1998 drought, it is not surprising to see that the National Centers for Environmental Prediction (NCEP) operational climate forecasts made in March 1998 failed to capture the unprecedented drought (Barnston et al. 1999). It is therefore important to establish the mechanisms that originated and maintained the drought in order to determine whether such a drought is actually predictable.

Recently, Hong and Kalnay (2000) introduced a new approach to identify the physical mechanisms associated with extratropical climate extremes, using both global and regional models. Impact studies of internal forcing in regional models (Hong and Kalnay 2000; Hong and Pan 2000) do not consider the change of large-scale patterns and their subsequent feedback. This lack of feedback on the large scale is actually an advantage when the regional feedback is the primary concern, because it is otherwise difficult to isolate the regional internal forcing within a global modeling framework. The tropical SST anomalies have a global-scale impact, whereas the impact of soil moisture anomalies is much more local. Therefore, in this study, which is an extension of Hong and Kalnay (2000), the impact of SST is investigated using a global atmospheric model, while a regional model is used to examine the role of the regional feedback due to soil moisture anomalies.

The surface climatological and atmospheric circulation patterns of the 1998 summer are reviewed in section 2. The hypotheses that we explore and the model setup for the different experiments are discussed in section 3. The global model is used to study the impact of both near and far SST anomalies, and of initial conditions, and the results are presented in section 4. The impact of soil moisture anomalies, using the regional spectral model (RSM) is discussed in section 5. Section 6 presents a table summarizing the quantitative impact of the forcings in our experiments.

2. Overview of the 1998 OK–TX drought

In this section we briefly review the characteristics of atmospheric circulation features associated with the drought over the OK–TX region, which we define as the region bounded by 29°–37°N, and 105°–91°W, which also includes Arkansas and Louisiana (see Fig. 2a, later). Barnston et al. (1999) made a detailed evaluation of the NCEP Climate Prediction Center's operational forecast skill and a comprehensive description of the general atmospheric circulation patterns and their regional impact is available in Bell et al. (1999).

a. Surface observations and the reanalysis products over OK–TX during 1998

Figure 1a shows the daily precipitation accumulated over OK–TX between 15 March and 15 September

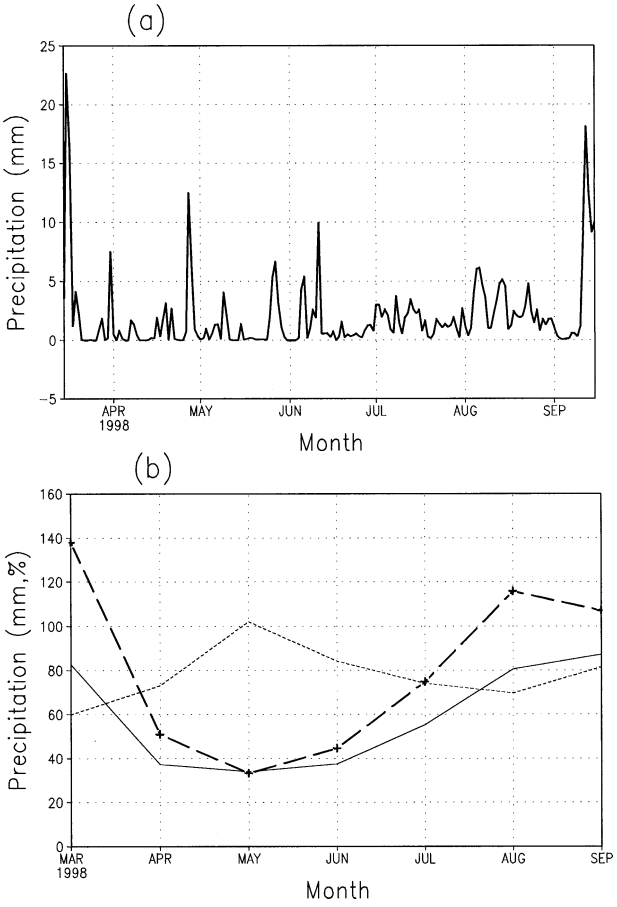

FIG. 1. (a) Daily observed precipitation averaged for the OK–TX area (29°–37°N, 105°–91°W) during 1998, (b) the comparison of monthly totals for 1998 observed precipitation (solid), climatology (dotted), and its ratio (thick dashed).

1998. They are obtained from the NCEP Climate Prediction Center (CPC) archive at 0.25° resolution. These were interpolated to a 1° resolution and monthly averaged to compare with the National Climate Data Center (NCDC) archives of monthly precipitation climatology at 1° resolution in Fig. 1b. Daily precipitation (Fig. 1a) shows heavy precipitation in mid-March. Very little rain was recorded for most of the period during April–June 1998, except for a few events causing significant precipitation on 30 March, 27 April, 28 May, and 5 and 10 June 1998. After 1 July, there was rain almost daily, but with moderate intensity. Heavy rain started to appear in mid-September. Figure 1b presents the observed and climatological monthly averages, as well as their ratio. March was 40% above normal. Below-normal precipitation began in April and the deficit was 65% in May, which is climatologically the month with the most precipitation. The ratio of the 1998 precipitation over the climatology is less than 50% during April–June, about 75% in July, and recovered the climatological value afterward.

Figure 2 presents the horizontal distribution of the precipitation anomaly over the continental United States. After above-normal precipitation over the OK–TX region in February and March 1998 (not shown), dryness started over the OK–TX region and Florida in April (Fig. 2a). May 1998 (Fig. 2b) is the mature stage of the drought over the OK–TX region (cf. Fig. 1b). The drought extends to Kansas and Missouri. Maximum deficit appears in southeastern Texas. Other regions in the United States show near-normal precipitation, except for the West Coast positive anomaly centered in northern California. In contrast to the water deficit in the southern part, flooding was recorded north of the drought region in June and July (Figs. 2c and 2d). The rainfall totals during April–June are less than 200 mm in broad sections of New Mexico, Oklahoma, Texas, and many locations across Florida, which is less than half the long-term average (Bell et al. 1999). In July, the drought ended in most regions, including Florida, New Mexico, Louisiana, and Arkansas. Over Oklahoma the water deficit was still distinct in August, but in southern Texas, floods were observed during that month (Fig. 2e). In September (Fig. 2f), most of the Gulf of Mexico states received above-normal precipitation, but dryness persisted throughout much of the OK–TX region. Despite the devastating intensity of the spring and summer drought, overall 1998 had average precipitation over Oklahoma because of the high amounts recorded during the first 3 months and after September 1998.

The surface precipitation and soil moisture obtained from the NCEP–National Center for Atmospheric Research (NCAR) reanalysis (Kalnay et al. 1996) are presented in Fig. 3. It is important to check whether the reanalysis anomalies in precipitation are reasonably realistic, since they determine the reanalysis soil moisture anomalies. In fact, the reanalysis 6-h forecast reproduces extremely well the amount and timing of the observed precipitation over the OK–TX region from April through the end of August (cf. Figs. 1a and 3a). The time correlation of area-averaged daily precipitation between the reanalysis and observations is as high as 0.79. The average intensity of precipitation during the analyzed period is also quite close (reanalysis has 2.26 mm day^{-1} vs observations of 1.96 mm day^{-1}). The estimated surface evaporation (Fig. 3a) indicates that there was an upward transport of near-surface soil moisture with moderate intensity of about 3 mm day^{-1}, resulting in a decrease of soil water for most of the spring and summer. Figure 3b shows the reanalysis climatological and 1998 soil moisture content of the two soil moisture layers in the model. Soil moisture at the thin top soil layer (0–10 cm) shows a synoptic-scale variation in response to precipitation activity, while the thicker bottom layer (10–200 cm) has a slow reduction of soil water in 1998 with a seasonal timescale. The soil water content at the top layer is smaller than the climatology for most of April–July, which is consistent with precipitation activities. The bottom layer soil responds slowly, with a lag of about a month, relative to the evolution of precipi-

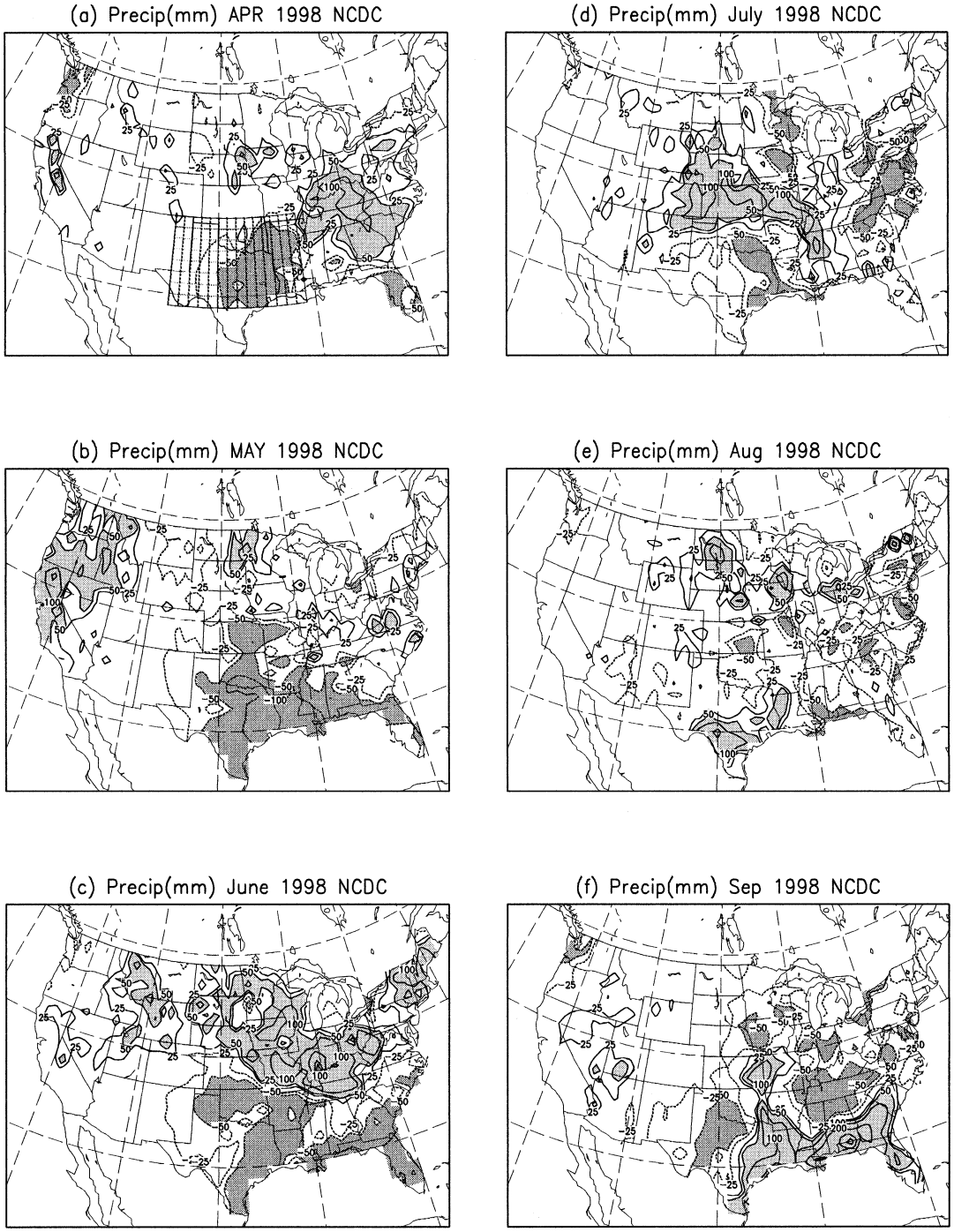

FIG. 2. Monthly precipitation anomalies from Apr to Sep 1998. Climatology is the average for 1949–98. A hatched area in Fig. 2a denotes the OK–TX area (29°–37°N, 105°–91°W) defined in this study.

tation. Because of the above-normal precipitation during March, the bottom soil is wetter than normal until early May of 1998. The bottom soil then dries in response to the long-lasting precipitation deficit. In mid-September, the amount of bottom soil water recovers the climatological value, due to the above-normal precipitation starting in mid-August. The 1998 drought was accompanied by record heat (Fig. 3c). The domain-averaged anomalies in temperature are as high as 3 K throughout May–July.

These and other comparisons with Basara et al. (1999) surface and soil observations from the Oklahoma Mesonet provide confidence that the reanalysis can indeed be used for initializing the model and for the verification

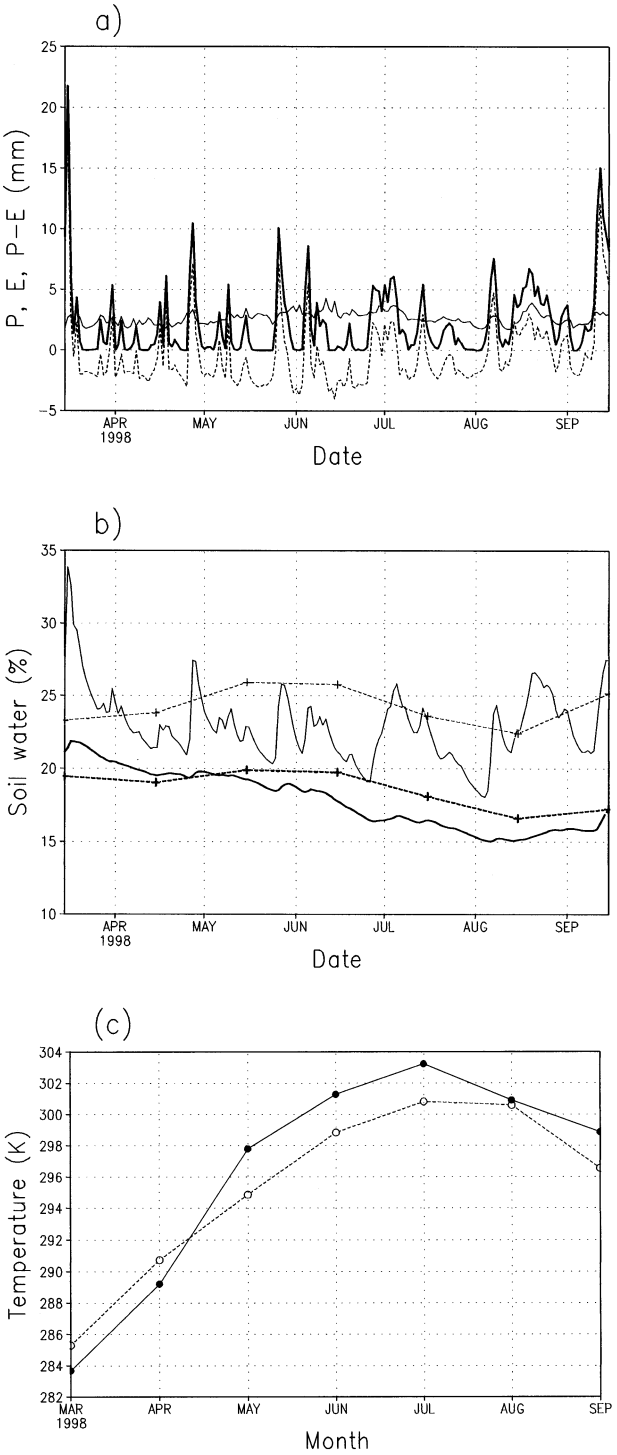

FIG. 3. Daily values averaged for the OK–TX area (29°–37°N, 105°–91°W) of (a) precipitation (*P*: thick solid), evaporation (*E*: thin solid), and precipitation minus evaporation (*P* − *E*: thin dashed), (b) daily soil moisture in 1998 (bottom layer: thick solid, top layer: thin solid), and the corresponding monthly climatology (bottom layer: thick dashed, top layer: thin dashed), and (c) monthly temperature (1998: solid, climatology: dashed), estimated from the NCEP–NCAR 50-yr reanalysis. Monthly climatology is the average during 1949–98.

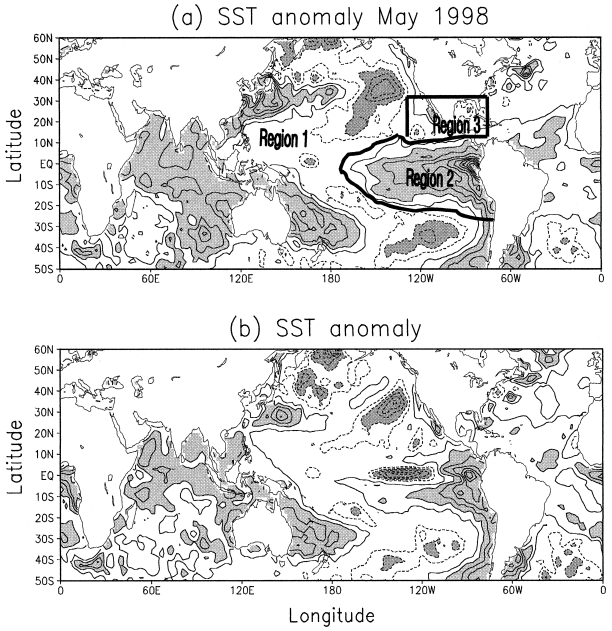

FIG. 4. SST anomalies averaged for (a) May and (b) Jun 1998. Three regions in (a) correspond to the experiments SMSST1, SMSST2, and SMSST3, in which the SST anomalies within the corresponding regions were used. Contour intervals are 0.5 K, and 0 K lines are omitted. Shaded are the absolute values greater than 1 K.

of the results, as well as for examining the circulation anomalies associated with the 1998 drought.

b. Large-scale circulation

We first present the SST anomalies for May and June 1998, a transition period between the record El Niño of 1997/98 and the quickly established La Niña episode in the second half of 1998. SST anomalies are obtained from the observations used in the 50-yr NCEP–NCAR reanalysis (Reynolds 1988). Although the warm SST anomalies in central and eastern Pacific observed during the 1997/98 winter were significantly weakened in the spring of 1998, the warm anomalies in eastern Pacific were still pronounced in May 1998 (Fig. 4a). Areas of the anomalies greater than 2 K are present east of 120°W, with the width of about 5°–10° latitude. Warm anomalies greater than 1 K cover much of the Indian Ocean and east of Australia. Horseshoe-shaped cold anomalies appear in the central and North and South Pacific. In June (Fig. 4b), strong cold anomalies appear over the equatorial Pacific between 160° and 110°W. These cold anomalies became stronger with time, but the warm anomalies in the far eastern Pacific remained present throughout the summer of 1998.

Many features of the atmospheric circulation pattern that had generally persisted from the previous winter broke down during July, signaling an end to the direct influence of the 1997/98 El Niño on North American weather patterns (Bell et al. 1999). During April–June

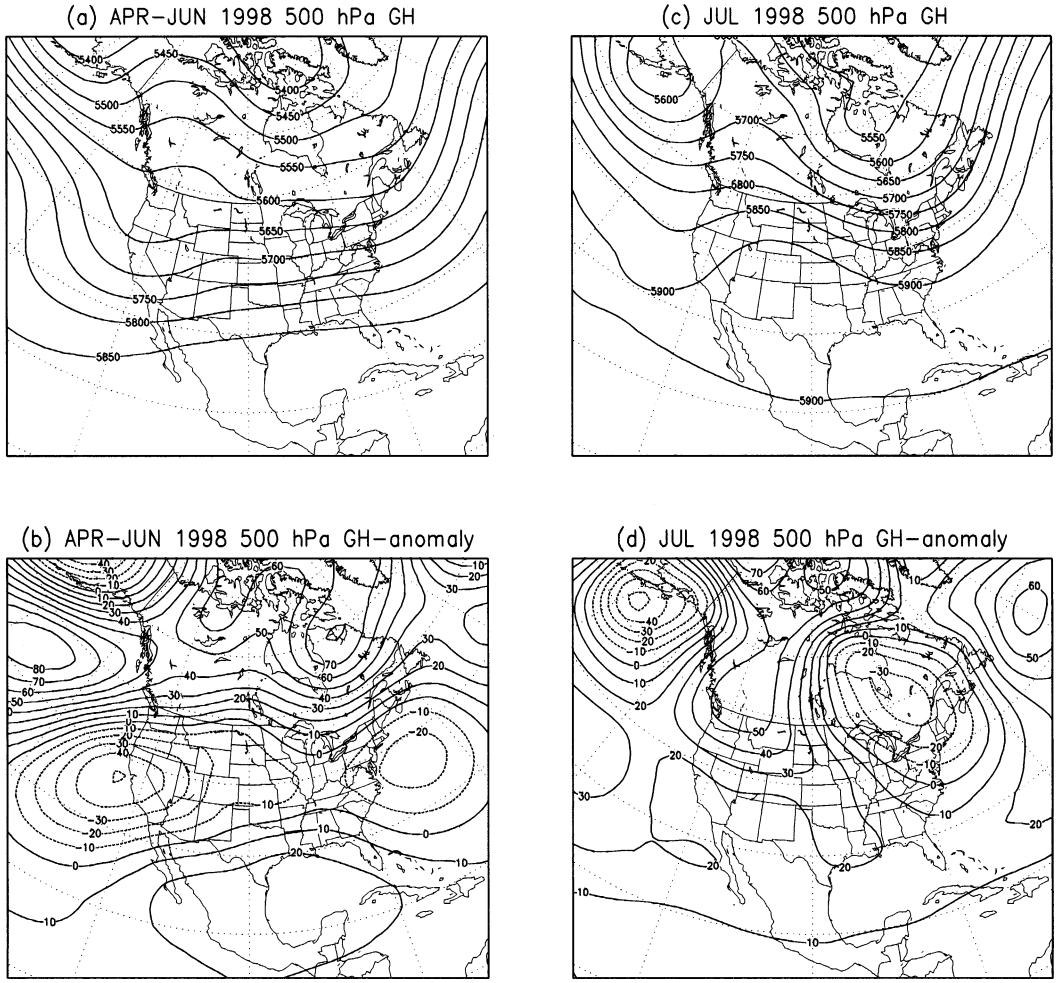

FIG. 5. 500-hPa geopotential heigh averaged for (a) Apr–Jun and (c) Jul 1998, and (b) and (d), their anomalies over the climatology during 1949–98.

(Figs. 5a and 5b), an anomalous ridge covered Mexico and the south-central United States, a trough prevailed near California and the western Atlantic, and the Hudson Bay low was weaker than normal. An unseasonably strong jet stream and increased storminess across central and northern sections of the continental United States accompanied this circulation pattern, related to above-normal precipitation that covered much of the western, midwestern, and northeastern portions of the United States in June and July (Figs. 2c and 2d). In July (Figs. 5c and 5d) a wavelike upper-level flow pattern prevailed, with ridges and troughs taking on a north–south orientation. An amplified ridge covered the south-central states and the west while an anomalously strong upper-level Hudson Bay low was evident across eastern North America.

Figure 6 shows a Hovmöller diagram (time–longitude cross section) for 500-hPa zonally asymmetric components of the waves (departure from the zonal mean) from 15 March to 15 September 1998. In the figure, APR1998 denotes the beginning of April. By mid-June when the El Niño signal remains, negative height anomalies were distinct between 130°–110°W and 80°–70°W. The former is associated with a stormy season in the West Coast, and the latter associated with a weakened subtropical high centered in the Atlantic. Between the two regions, positive anomalies appear centered at 95°W. In April, the positive anomaly in relation to the drought is not pronounced, but the magnitude of anomalies over the drought region, between 100° and 90°W, is relatively low. A well-organized ridge began to appear on 10 May 1998. This ridge is distinct until early August, even after the El Niño–related upper-level circulations faded in mid-June. Cause and effect cannot be determined by a simple diagnostic, but this and circulation features in Fig. 5b imply that the drought from April to mid-June could be a direct influence of the El Niño, but such a long-lasting nature is likely to reflect internal atmospheric variability such as a local feedback in the OK–TX region, and not the influence from either lingering El Niño or developing La Niña conditions.

In relation to the inquiry to why the late spring

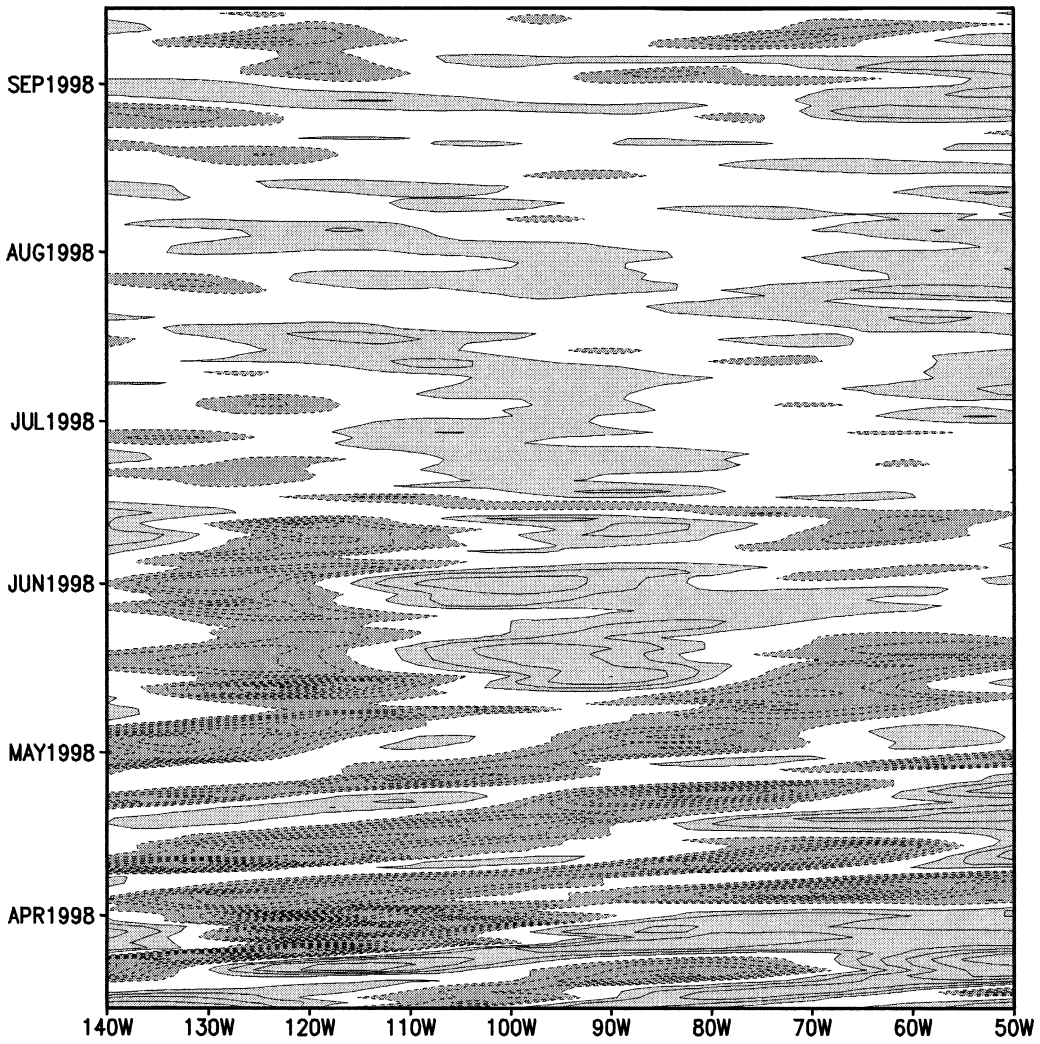

FIG. 6. Hovmöller diagram of quasi-stationary waves for 500-hPa heights averaged over the latitudes 29°–37°N, from 15 Mar to 15 Sep 1998. Shaded areas have absolute values greater than 30 m; contour intervals are 30 m, and 0-m lines are omitted.

drought in the South occurred, running counter to the historical El Niño composite, Bell et al. (1999) noticed the particular manner in which the El Niño ended. Although it ended abruptly across much of the tropical Pacific in very late May 1998, the SST in the far eastern tropical Pacific (80°–105°W) remained well above normal throughout the summer (see Fig. 4). In late spring 1998 the subtropical ridge in the north, with the remaining anomalous tropical convection over the lingering warm waters in the eastern Pacific, migrated northward into the southern United States in association with the normal seasonal solar progression. As noted in Barnston et al. (1999), the above hypothesis might be challenged since the drought started in April, before the warm SST became limited to the far eastern Pacific basin.

3. Hypotheses and numerical experimental setup

a. Hypotheses

We have already seen that the establishment of the drought during April–May 1998 could not have been due to soil moisture anomalies. The soil was wetter than normal until early May 1998 due to above-normal precipitation in early spring (Fig. 3b). For this reason, we proposed and tested numerical experiments with the following hypotheses: (i) the waning warm ENSO episode in the early spring of 1998 helped to establish the anomalous OK–TX drought conditions during the spring of 1998, and (ii) the consequent deficit in the soil moisture contributed to maintain the drought throughout the summer and early fall through a local positive feedback between the atmosphere and the land. Because the two

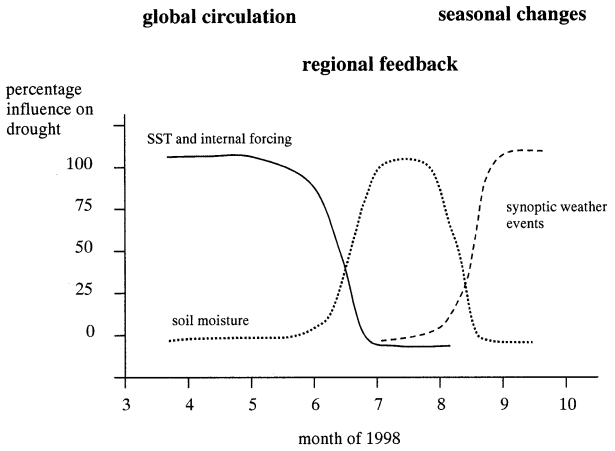

FIG. 7. Schematic of the conceptual physical mechanisms that dominated the origin, maintenance, and demise of the OK–TX drought of 1998.

mechanisms invoked for the drought establishment during the spring and its maintenance during the summer are quite different, we need different modeling approaches to test the two hypotheses. To test the first hypothesis where it is necessary to allow for global-scale SST forcings, we integrated the NCEP global spectral model (GSM) with climatological and observed SSTs. For the second hypothesis, based on regional feedbacks, we needed to maintain the observed global circulation close to observed, so that we opted for running the NCEP RSM, using the NCEP–NCAR reanalysis as lateral boundary conditions. The third mechanism, that the initial atmospheric circulation was favorable to the drought even in the absence of surface boundary forcing, is acting implicitly through the use of observed (reanalysis) initial conditions, and is tested within the GSM framework.

Figure 7 displays schematically the conceptual hypotheses discussed above. In the rest of the paper we test whether these hypotheses are supported by the regional and global-scale experiments.

b. Description of the global spectral model experiments

The GSM used in this study has the same physics as the NCEP medium-range forecast (MRF) model operational as of January 1998, but with some modifications in the parameterized convection. The introduction of an enhanced evaporation of falling precipitation in the parameterized convection over the oceans produces a more realistic distribution of precipitation in the Tropics in response to SST anomalies (Hong 2000). A more detailed description of the MRF is available in Caplan et al. (1997). The version of the model used in this study has a horizontal resolution corresponding to the spectral truncation of T62 (triangular truncation at wavenumber 62, equivalent to about 200-km horizontal resolution) and a vertical resolution of 28 layers in the sigma coordinate system. Given a proposal based on the fact that lingering warm SST anomalies in the far eastern Pacific during the dissipation stage of the 1998 ENSO episode can be associated with the unprecedented drought and heat waves in the OK–TX region, and that the month of May 1998 was a transition period from the El Niño to La Niña, we decided to focus on the experiments for the month of May 1998. To check the influence of boundary conditions (SST and SM), we computed ensembles of five lagged average forecasts (LAF; Hoffman and Kalnay 1983) starting on 26, 27, . . . , 30 April 1999, at 0000 UTC, and verified during the month of May 1998. This is in order to filter out weather noise, and to check the statistical significance of the results. Four separate experiments were run for May 1998:

- SMSST: 1998 reanalysis soil moisture and 1998 observed SST,
- SM: 1998 reanalysis soil moisture and climatological SST,
- SST: 1998 observed SST and climatological soil moisture,
- CLIM: climatological SST and soil moisture.

For the control experiment, SMSST, we used the NCEP–NCAR 50-yr reanalysis to create initial atmospheric and soil moisture conditions. Observed SST were updated every 24 h. In the CLIM and SM experiments, monthly climatology of SST data during 1949–98 is linearly interpolated at model integration time. The soil moisture was predicted from the land surface model during model integration. The SM experiment replaces the observed SST by a climatological SST during 1949–98, whereas in the SST experiment soil moisture at model initial time is derived from reanalysis climatology also for the period 1949–98. The CLIM experiment uses climatological values for both SST and soil moisture at the initial time. Note that soil moisture anomalies are applied to all land points over the entire globe. The same ensemble experiments designed for May were extended for April and June starting at the end of March and May, respectively, and their results will be briefly discussed in the final section of this paper.

Additional experiments are designed to further examine the impact of SST anomalies and the importance of atmospheric internal forcing. During May 1998, the SST anomalies were in transition between the strong 1997/98 strong El Niño and the La Niña that established itself in the summer (Takayabu et al. 1999). Figure 4a shows the boundaries of three regions: the region marked 2, between 10°N and 28°S latitude, and 170°–70°W, contains the still strong warm SST anomalies associated with El Niño. We denote as region 1 the complement of region 2, that is, the global SST anomalies outside region 2. Region 1 includes the horseshoe-shaped cold anomalies that frequently appear in the central and North and South Pacific during a transition to

TABLE 1. Summary of experimental designs. A dash means the same setup as in the SMSST and CTL for global and regional experiments, respectively.

Model	Code	Soil moisture	SST	Initial atmospheric conditions
MRF	SMSST	1998 reanalysis	1998 observed	1998 reanalysis
	SM	—	Climatology	—
	SST	Climatology	—	—
	CLIM	Climatology	Climatology	—
	SMSST1	—	1998 observed within region 1 of Fig. 4a	—
	SMSST2	—	1998 observed within region 2 of Fig. 4a	—
	SMSST3	—	1998 observed within region 3 of Fig. 4a	—
	1993	1993 reanalysis	—	1993 reanalysis
RSM	CTL	1998 reanalysis	1998 observed	
	CLM	Climatology	—	
	DRY	Wilting point	—	

La Niña (M. Richardson 1999, personal communication). Region 3 is included within region 1 and limited by 10°–35°N, and 80°–140°W, and contains the cold anomalies centered in the Gulf of Mexico and at 15°N–120°W. We performed several additional experiments denoted SMSST1 (including soil moisture anomalies, and all SST anomalies within region 1, SMSST2, with SST anomalies within region 2, and SMSST3, with SST anomalies only within region 3 (see Fig. 4a). Another experiment is designed to investigate the role of initial atmospheric conditions. The 1993 experiment uses the SST of May 1998, but with soil moisture and atmospheric conditions for 1993 at the model initial time. This experiment will explore the importance of the SST anomalies in 1998 to the development of the drought.

c. Description of the regional spectral model experiments

Although the impact of soil moisture can be explored in a global model, it is difficult to isolate the local feedback because the large-scale circulation can also change within a global forecast. Thus, in order to test the second hypothesis, a local feedback between soil moisture and precipitation, the reanalysis boundary conditions were used to drive the NCEP RSM (Juang et al. 1997). This approach has the advantage that the large-scale circulation remains very close to observations, since it is substantially determined by the reanalysis lateral boundary conditions, whereas local feedback between soil moisture and precipitation is still allowed to vary from experiment to experiment. The performance of the NCEP RSM for regional climate modeling has been evaluated in Hong and Leetmaa (1999), Hong et al. (1999), and Hong and Pan (2000). Hong and Leetmaa (1999) and Hong et al. (1999) have shown that the model resolved small-scale features embedded within a large-scale circulation without a discernible synoptic-scale drift. Hong and Pan (2000) demonstrate that given the same large-scale forcing the model has considerable freedom in response to internal forcing compared with other regional models. Hong and Pan (2000) also have shown that the model exhibits a distinct positive feedback between soil moisture anomalies and precipitation even in the small domain, unlike the results of Seth and Giorgi (1998). This uniqueness is partly due to the nesting strategy as a ''domain nesting'' in physical space as well as a ''spectral nesting'' in spectral space, instead of the conventional ''lateral boundary nesting'' as used in most regional models. In the RSM, the large-scale wave longer than the regional domain from the coarse grid or global model cannot be disturbed. Further details on this issue are available in Juang and Hong (2001).

We located the model domain centered in the OK–TX region, with a nominal horizontal resolution of 50 km. The number of grid points in Cartesian coordinates is 65 (west–east) by 44 (north–south). This domain is the same as the small domain used in Hong and Pan (2000), but farther displaced southward by about 5° to latitudes covering northern Mexico. Initial conditions were obtained from the reanalysis. The lateral boundary conditions and base fields were linearly interpolated in time from the 6-h reanalysis data. Observed SSTs were updated every 24 h. The 6-month-long simulations began on 0000 UTC 1 April 1998. In the RSM, only the bottom (deep) soil moisture model layer (10–200 cm) is updated from the reanalysis every 24 h during the model integration period, while the soil moisture in the top (shallow) layer is predicted. This is because the top soil layer (0–10 cm) interacts directly with the atmosphere and needs to be therefore in balance with the atmospheric forcing.

Three types of runs with different soil moisture over the RSM domain designed were: CTL, with soil moisture taken from the reanalysis soil moisture for 1998; CLM, with climatological soil moisture from the reanalysis for the period 1949–98; and DRY, with soil moisture values at the wilting point.

All experiments conducted in this study are summarized in Table 1.

4. Results from the global experiments: SST anomalies

To assess general skill of the various sensitivity experiments performed in this study, we first verified the

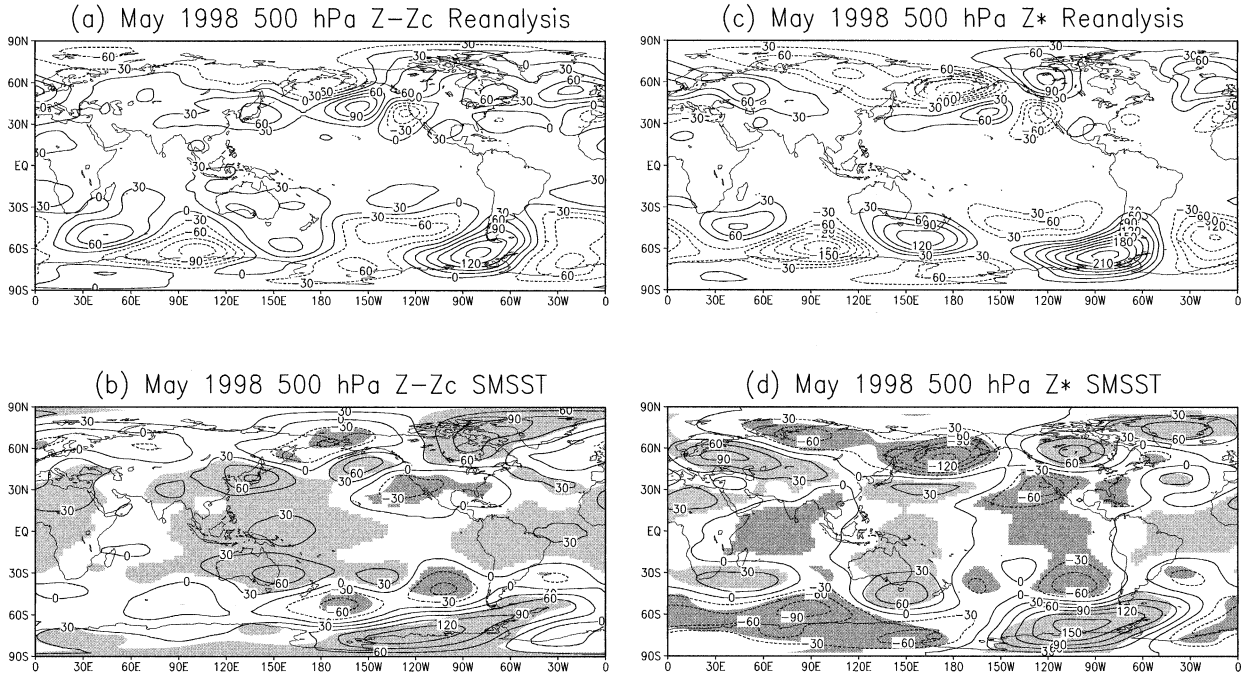

FIG. 8. Monthly 500-hPa height anomalies for May 1998 from (a) reanalysis, (b) the average of five-member ensembles from SMSST experiment, (c) and (d) the corresponding quasi-stationary waves. Shaded areas in (b) and (d) have a level of significance greater than 95%.

global climatology resulted from the control experiment. A comparison of simulations with observed and climatological SST will be focused on the differences in the simulations with observed soil moisture (SMSST − SM). The regional impact over the OK–TX region is investigated from the 10-member ensembles: observed SST (OSST: SMSST + SST), climatological SST (CSST: SM + CLIM), observed soil moisture (OSM: SMSST + SM), and climatological soil moisture (CSM: SST + CLIM).

Statistical *t* tests were performed to address the significance of the ensemble members. From the n members, we can define $t = |\overline{x}/\sqrt{s/(n-1)}|$ where $\overline{x}$ is the mean departure from climatology and s is the variance. Each member is assumed to have one degree of freedom. For five members ($n = 5$, 4 degrees of freedom), the statistic t needs to be over 2.13 and 2.78 for $\overline{x}$ to be statistically significantly different from 0 at the 90% and 95% significance level, respectively. To address the extent to which the SST or soil moisture anomalies have a significant impact on the simulated signals, the difference map between the ensemble means should be considered. To check the statistical significance of the difference, we computed the t value by assuming that the data follow the normal distribution. If $\overline{x}_1$ and $\overline{x}_2$ are the two sample means, and s_1 and s_2 are the variances for sample 1 and 2, then the value, $t = |(\overline{x}_1 - \overline{x}_2)/\sqrt{(s_1 + s_2)/(n-1)/2}|$. For $n = 5$, the t value needs again to be over 2.13 and 2.78 for the difference of the ensemble means to be different at the 90% and 95% significance level, respectively. For $n = 10$, the value of t needs to be over 1.83 and 2.26 for the difference to be statistically significant at the 90% and 95% significance level, respectively.

a. The control experiment (SMSST)

The 500-hPa heights from the SMSST experiment are compared with the reanalysis in Figs. 8a and 8b. The May climatology from reanalysis during 1949–98 is taken out from both forecasts and analysis to form anomalies. In principle, to obtain model anomalies we should subtract the monthly model climatology from the model integration, but since it is not available, we subtract the reanalysis climatology. Despite these uncertainties, the performance of the control experiment (SMSST) is in general good in both the NH and SH in terms of patterns. The comparison between Figs. 8a and 8b indicates that the model has zonal mean biases associated with a model drift and the quasi-stationary waves (Figs. 8c and 8d) are therefore somewhat better simulated than the total anomalies. The quasi-stationary wave component at a grid point is defined as the time-averaged departure of the value from the zonal mean at the same latitude. The wave train over North America is fairly well simulated in location and intensity (Figs. 8c and 8d). Even the features in Europe and Asia are reproduced well, where the influence of the SST anomalies in the tropical Pacific is weak. Most centers of the wave train in the Pacific North America (PNA) region are statistically significant,

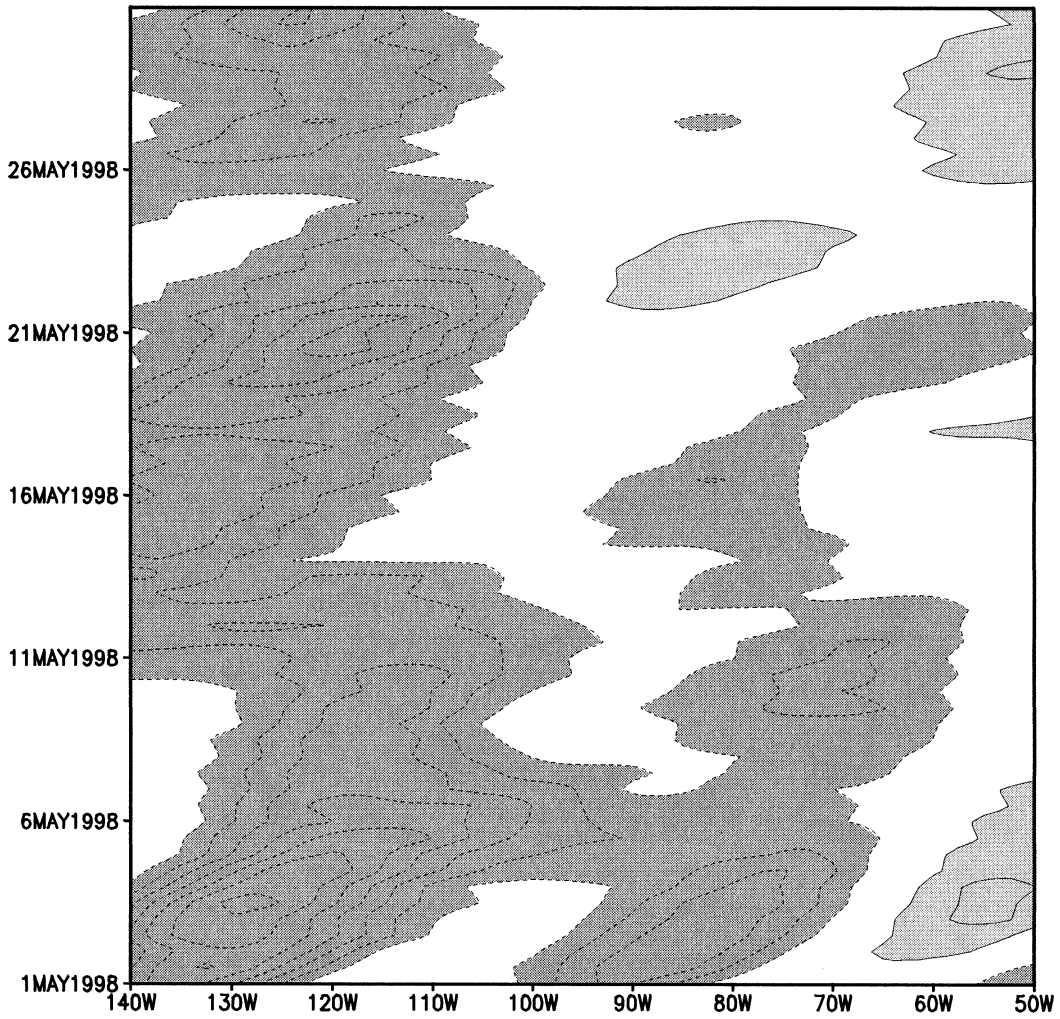

FIG. 9. Same as in Fig. 6, but for the ensemble average of five-member SMSST experiments during 1–31 May 1998.

and the significance is higher in the standing waves. In the northern Atlantic the model does not reproduce correctly the anomalies. In the SH, simulated height patterns show a general agreement with the corresponding observations, but with weaker magnitudes. To objectively assess the skill of the control simulations, the anomaly correlations and root-mean-square errors (rmse) for the ensemble mean were computed. Anomalies were defined as deviations from the May climatology (Figs. 8a and 8b). The anomaly correlation of the ensemble mean of the simulated 500-hPa heights over the PNA region (10°–60°N; 170°–60°W) is as high as 0.91. The correlations over the globe, the NH, and the midlatitude (30°–60°N) are 0.53, 0.59, and 0.68, respectively. The area-averaged rmse shows a minimum of 21 m in the NH, and maximum of 26 m in the midlatitudes.

Figure 9 shows the Hovmöller diagram of quasi-stationary waves for 500-mb heights averaged over the OK–TX latitude belt from the SMSST experiment. In comparison with the analysis (Fig. 6), the model simulates well the evolution of two negative anomalies centered in 130°–120°W, and 85°–75°W in terms of timing, but the magnitudes are weak. Onset of the near-zero or weakly positive anomaly between the two negative anomaly regions at around 7 May compares well with the observation. The model reproduces long-lasting negative anomalies in the western region and decay of another negative anomaly to the east of the OK–TX region. However, the magnitude of these anomalies is weaker by a factor of 1–3.

b. Impact of the SST anomalies

In Fig. 10, the ensemble mean precipitation difference between SMSST and SM experiments is compared with the observed anomaly for 1998. The monthly simulated precipitation in the figure is the average of the five-

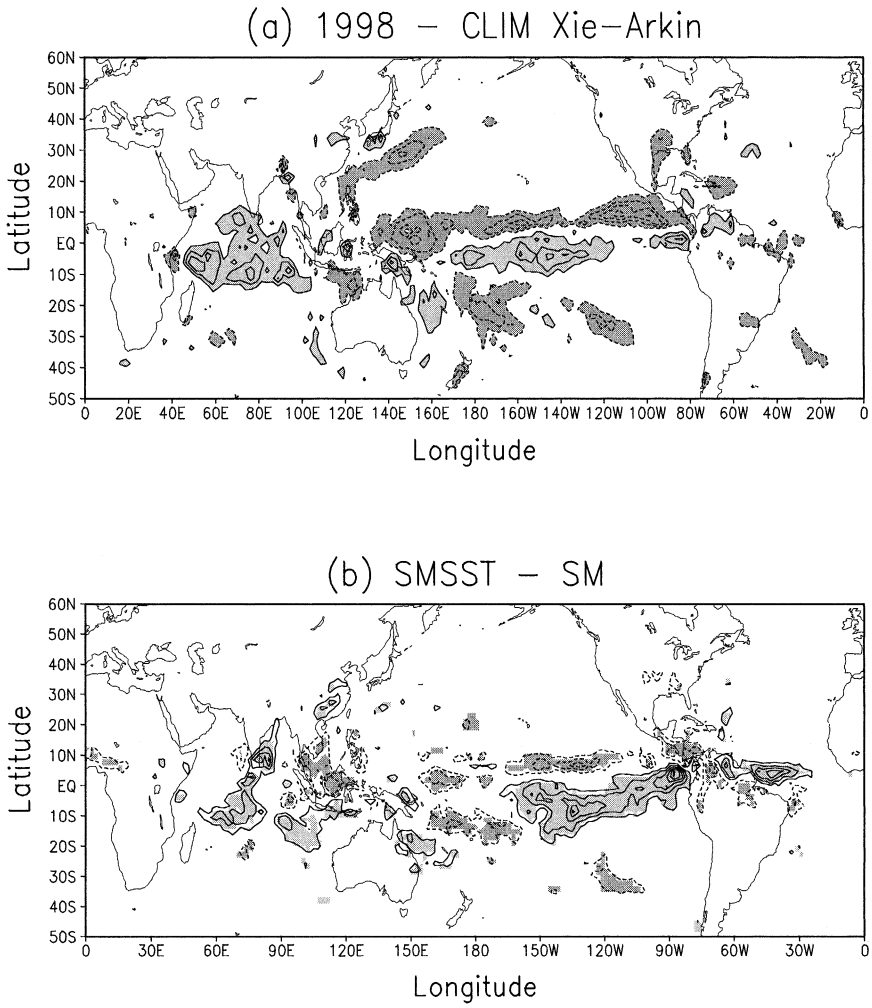

FIG. 10. (a) Analyzed precipitation anomalies relative to the climatology for 1979–98 from Xie and Arkin (1996), and (b) simulated precipitation anomalies (SMSST − SM). Contour intervals are 100 mm without zero lines. Shaded areas in (a) have absolute values greater than 100 mm, (b) for the significance greater than 95%.

member ensemble forecasts. The model is able to reproduce much of observed pattern over the Tropics in response to the SST anomalies (Fig. 4a), including positive anomalies over the tropical central and eastern Pacific, and over the Indian Ocean. The center of positive anomaly in the central tropical Pacific is shifted to the east by about 30°. The horseshoe-shaped pattern of negative anomalies surrounding the positive anomalous region over the tropical Pacific are well reproduced, but with weaker intensity. The general underestimation of anomaly suggests that the observed SST anomaly associated with a warm ENSO episode alone is not enough to account for the anomalous precipitation, even in the tropical oceans during May 1998. It is also noted that little representation of the drought over the OK–TX region is seen in Fig. 10b, but it is clearer in the larger ensemble anomaly that will be discussed at the end of this section.

The influence of SST anomalies on midlatitude atmospheric circulation is presented in Fig. 11. The magnitudes of height anomalies due to SST anomaly are much smaller than the observed anomalies (cf. Figs. 8a and 8c). However, the relatively significant anomalies over the PNA region are attributable to SST anomaly. A positive anomaly centered at 30°N, 160°W; weak negative at 25°N, 130°W; a negative in the southeastern United States; and a positive in northeastern North America are comparable to the observed features. It is important to note that although the anomalies over the PNA regions are weak and are not statistically significant, they are responsible for the midlatitude teleconnection due to the tropical SST anomalies, which in turn

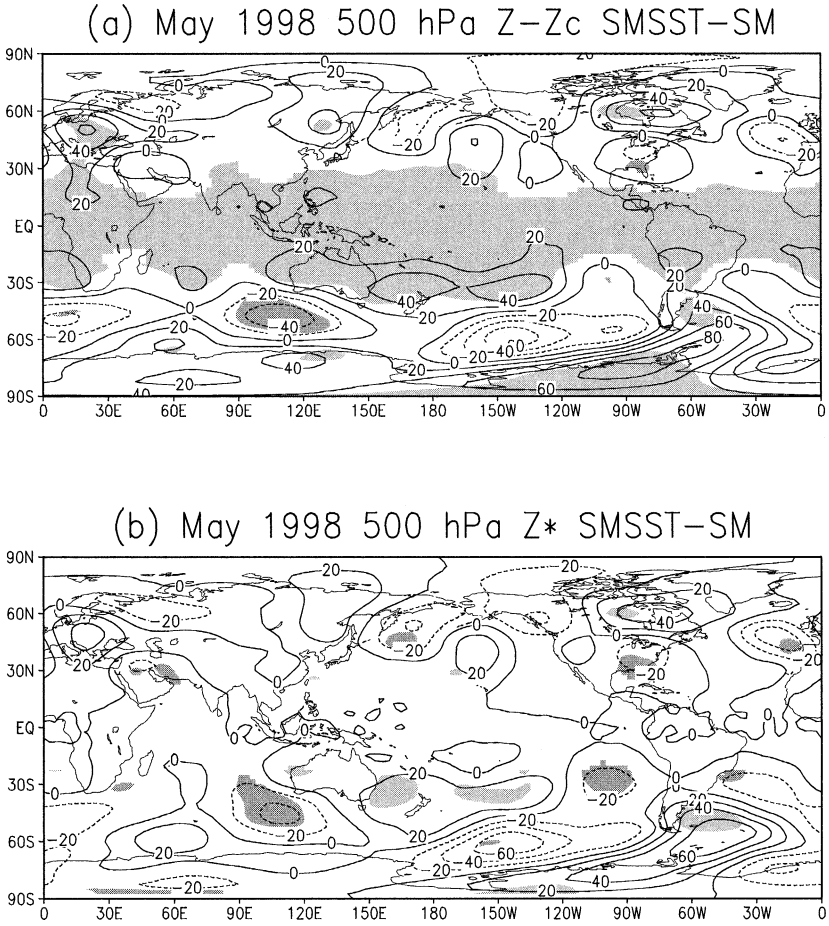

FIG. 11. Difference map between SMSST and SM experiments of (a) 500-hPa height and (b) quasi-stationary waves. Areas where features are statistically significant at the 90% level are shaded.

reduces the low-level jet from the Gulf of Mexico, as will be discussed in the following. Figure 12 shows the impact of both SST and soil moisture anomalies on the OK–TX precipitation and moisture fluxes. The number of degrees of freedom for the precipitation ensembles is estimated as 9 for the precipitation (since the ensembles have 10 members), and as about 30 for the moisture divergence, since the latter is computed from daily values. The twice-daily data averaged from 10-member ensembles are used to compute the moisture convergence. Thus, the number of degrees of freedom for the selected dataset is estimated as 62, but it can be halved by neglecting diurnal variation. The observed precipitation (Fig. 11a) is that of Xie and Arkin (1996) since it also includes estimates over the ocean. Figure 12 is one of the main results of this paper: it shows that the impact of the SST anomalies (OSST − CSST) on the precipitation during May is very large and clearly contributed significantly to the establishment of the drought over OK–TX (Fig. 12b). Note that the drought signal is distinct as ensemble number is doubled (cf. Figs. 10b and 12b). The precipitation response to SST anomalies compares very well with the observed drought except for a slight shift to the east. Very importantly, the low-level moisture advection and convergence anomalies reveal similar flow patterns for both observations and model simulations (Figs. 12d and 12e), and suggest that the drought was a result of a reduced low-level jet and moisture transport from the Gulf of Mexico into the OK–TX region.

Meanwhile, it can be deduced that a west–east pressure gradient force in Fig. 11, which is a combined effect of the positive height anomaly centered at 30°N, 160°W and the negative anomaly center located in the southeastern United States, is responsible for a weakened moisture transport from the Gulf of Mexico to the north. It is well known that the low-level jet from the Gulf of Mexico into the gulf states is responsible for much of the transport of moisture into the eastern United States, and this reduction of the low-level jet intensity associated with the SST anomalies has apparently had an important impact upon the generation of the drought.

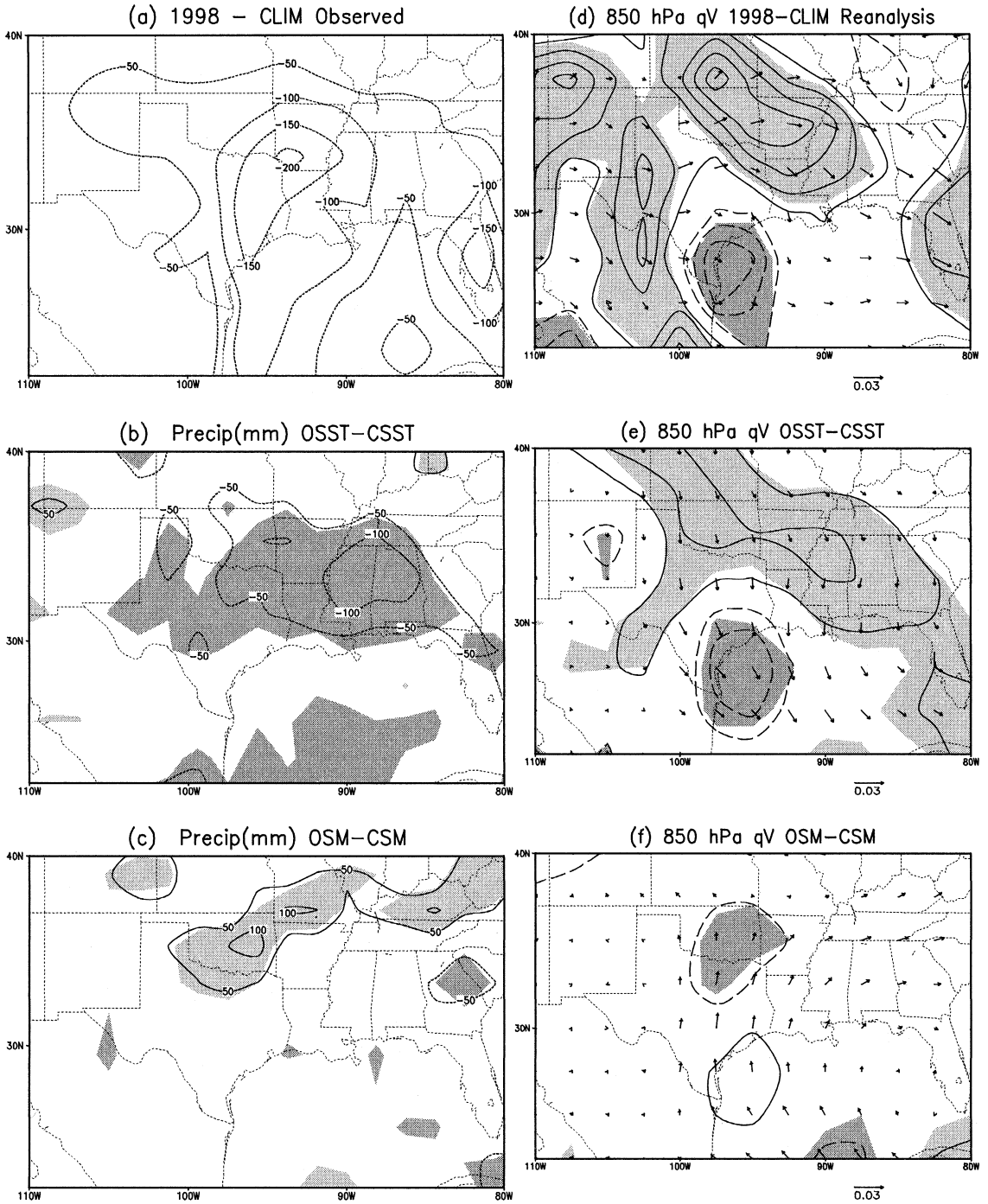

FIG. 12. (a) Analyzed precipitation anomalies from Xie and Arkin (1996), and the simulated anomalies: (b) OSST − CSST, (c) OSM − CSM. (d)–(f) The corresponding 850-hPa moisture divergence (lines) and moisture advection (vector). Shaded areas have features statistically significant at the 95% level.

Figure 12 also shows that, during May 1998, the impact of the soil moisture was to enhance precipitation in the OK–TX region, by increasing the low-level moisture transport from the Gulf. This enhanced precipitation is due to above-normal soil moisture anomalies at the end of April in which the model is initialized (see Fig. 3b). From the spatial distribution of the soil moisture anomalies at the model initial time (not shown), above-normal anomalies appear in the northern part of the OK–TX region where positive precipitation anomalies are simulated in Fig. 12c. This implies that the effect of soil moisture anomalies over the globe is largely local,

as found in previous studies (Wang and Kumar 1998; Fennessy and Shukla 1999). Another reason for positive precipitation anomalies associated with enhanced northerly flow in the soil moisture experiments can be associated with wet soil moisture anomalies in the western United States at the end of April. Meanwhile, the fact that the observed moisture flux anomaly is less southerly in the observations (Fig. 12d) than in the SST anomaly experiments (Fig. 12e) is probably due to the fact that in the real atmosphere they were moderated by the opposite soil moisture impact (Fig. 12f). As we indicated before, the local impact of soil moisture anomalies is difficult to quantify in the global model framework because of changes in the regional circulation. This impact will be further addressed in the regional model framework.

Our sensitivity experiments indicate that the SST anomaly played a positive role in initiating the OK–TX drought, but it is not certain which part of SST anomalies played a major role in the establishment of the drought. Also, note that the change of precipitation due to SST anomalies (SMSST vs SM), 35%, is smaller than in the observation, 65%. This implies that initiation of drought may be partially attributable to ''internal forcing,'' that is, to atmospheric initial conditions in early spring of 1998. This will be further addressed in section 4d.

c. Impact of far and near SST anomalies

We now discuss the results of experiments where only the far (region 1) or the near (region 2) Pacific SST anomalies, or where only the cold anomalies in the Gulf of Mexico and off Central America (region 3) are included. Figure 13 shows the changes of precipitation and 850-hPa moisture convergence with a wind vector produced by the three experiments (SMSST1, SMSST2, and SMSST3), relative to the SM experiment. The changes in the tropical precipitation are negligible in the SMSST1 and SMSST3, whereas the pattern from the SMSST2 preserves much of the tropical Pacific anomalies seen in the SMSST experiment (not shown). From Fig. 13, it is apparent that region 1, region 2, and region 3 SST anomalies all contribute to the drought in a similar way as in the impact of global SST anomalies (OSST–CSST). The 500-hPa anomalies (not shown) indicate an enhanced west–east pressure gradient in the Midwest resulted in an anomalous northerly flow toward the Gulf of Mexico. The corresponding reduction in the transport of moisture from the Gulf to the Midwest and consequent contribution to the drought is very apparent in Figs. 13d–f. The enhanced west–east pressure gradients were the result of different pressure anomalies in the three experiments. The far SST anomalies of region 1 resulted in a positive height anomaly centered at 30°N, 160°W, and a weak negative anomaly at 25°N, 130°W. The warm eastern Pacific SST anomalies of region 2 contributed instead to the reduction of heights in the southeastern United States. The cold SST anomalies in the Gulf of Mexico (region 3) also contributed to negative anomalies in the southeastern United States, but the impact was confined to the Gulf coasts. It is interesting to note that the drought is still significant without the SST anomalies associated with ENSO in the central and eastern Pacific (cf. Figs. 12b and 13a). It indicates that the warm ENSO SST anomalies alone did not initiate the drought. This is contrary to a physical scenario given by Bell et al. (1999). Rather, the impact of the warm ENSO SST anomalies (region 2) is as weak as that due to the cold SST anomalies in the Gulf of Mexico (region 3).

d. Impact of the initial conditions of the atmosphere

Finally we explore now the impact of the initial conditions, and the extent to which they were favorable to droughts or floods even in the absence of SST anomalies. Figure 14a shows precipitation anomalies due to atmospheric initial conditions corresponding to May 1993 rather than May 1998, but with SST and soil moisture anomalies as in 1998. There is no indication of the drought in the southern United States in the 1993 experiment. Rather, positive precipitation anomalies extending from the Texas Panhandle to the north show a similar pattern to that observed in May 1993. The reduction of precipitation in the northeastern United States is also comparable to what was observed in May 1993. The upper-air atmospheric conditions over the North American region were far from the pattern in May 1998, and much of precipitation anomalies in the Tropics related to anomalous SST distribution in May 1998 were weakened by increasing the precipitation amount along the equatorial Pacific between 100°E and 100°W (not shown).

This experiment emphasizes the importance of the initial conditions, also pointed out by Mo et al. (1991) for the 1988 Great Plains drought. Although this experiment shows the importance of the atmospheric structure expressed in the initial conditions, the impact of the SST anomalies cannot be separated out: the initial conditions are the result of the evolution of the atmosphere that has been subjected to SST anomalies during the previous months.

5. Results from the regional spectral model: Impact of soil moisture anomalies

Figure 15 shows the responses of precipitation and temperature due to soil moisture anomalies, derived from the RSM. The experiment with observed soil moisture in 1998 produced slightly above-normal precipitation in April, and near-normal in May. It is noted that the increase of precipitation in May is larger in the global model framework than that from the RSM (cf. Fig. 12c). As discussed in section 4b, a reason for larger impact in the global seems to be associated with significant wet soil moisture anomalies in the western Unit-

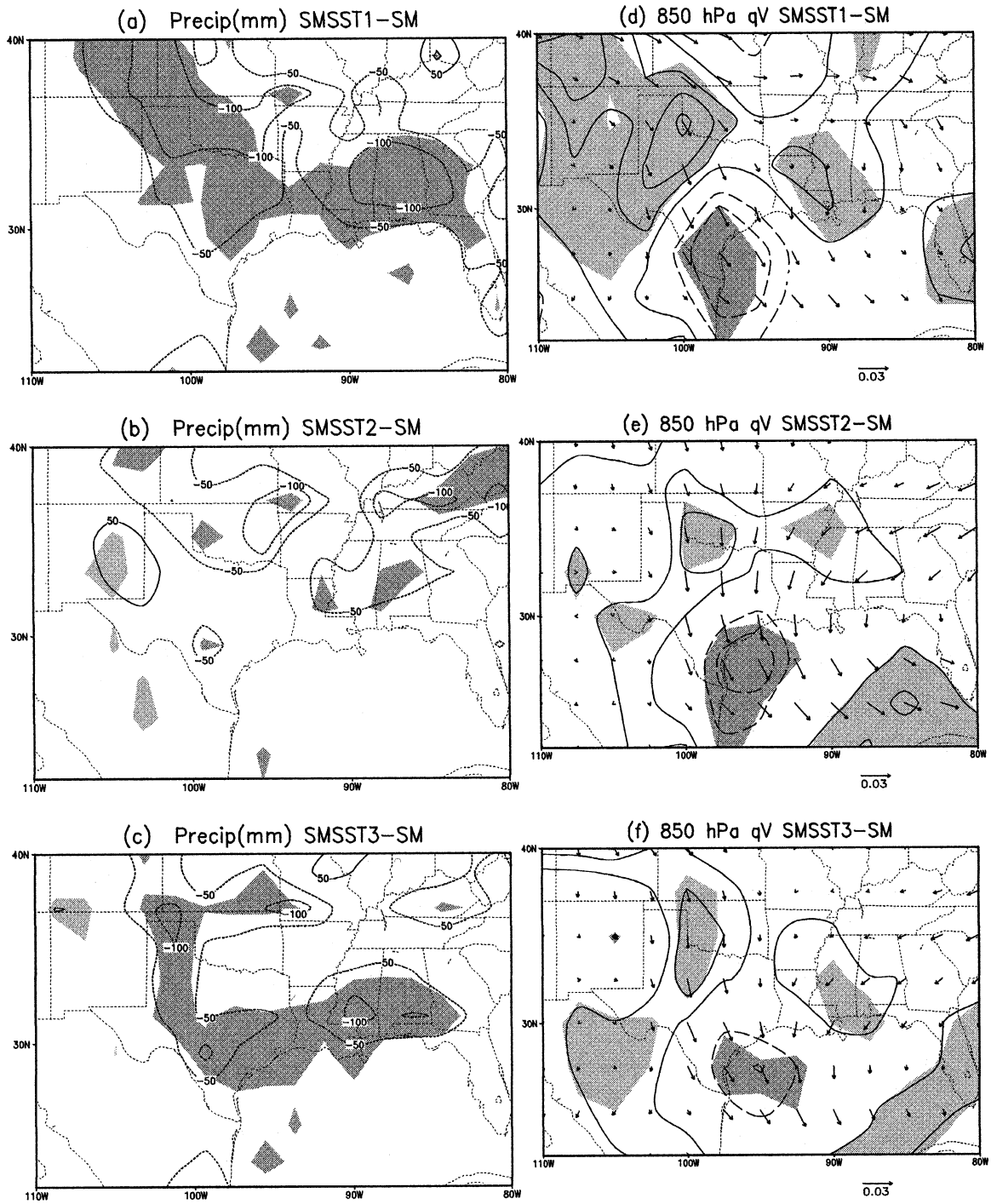

FIG. 13. Same as in Fig. 12, but for the SMSST1, SMSST2, and SMSST3 experiments.

ed States in relation to heavy rainfall in previous months. This area was excluded in the RSM framework. Another reason seems to be due to the decrease of soil moisture in May (see Fig. 3b). Note that the RSM simulation updates deep soil moisture daily, whereas in the global model the soil moisture is predicted after initialization.

The initial deficit in precipitation during April and May resulted in drier than normal soil wetness during these months over the OK–TX region. Dryness due to soil moisture anomalies becomes significant in June and is maximized in July. Soil moisture anomaly alone explains most of the deficit in July. The ratio of precipitation of 1998 against the July climatology is about 75%,

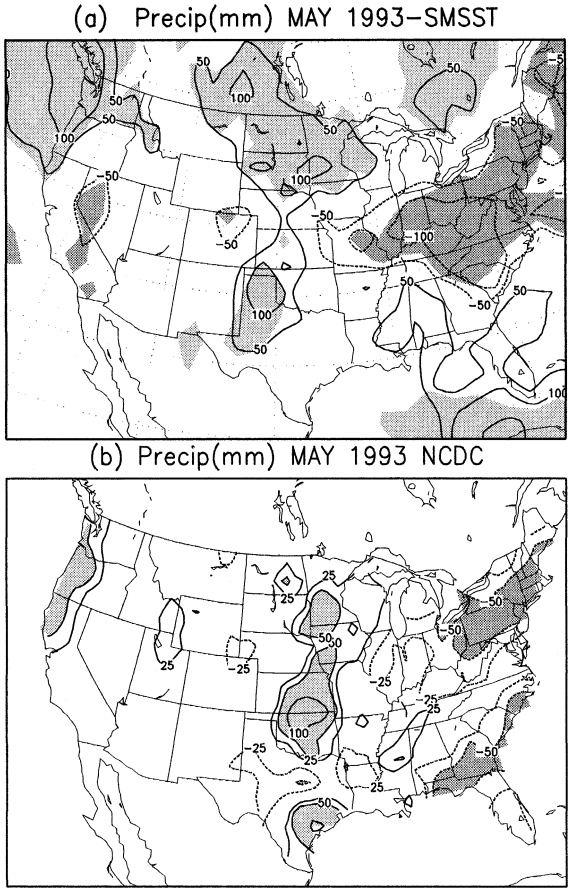

FIG. 14. (a) Precipitation difference between the 1993 and SMSST experiments, and (b) the observed anomalies in May 1993. Areas where features are statistically significant at the 90% level are shaded in (a). Shaded areas in (b) designate absolute values greater than 50 mm.

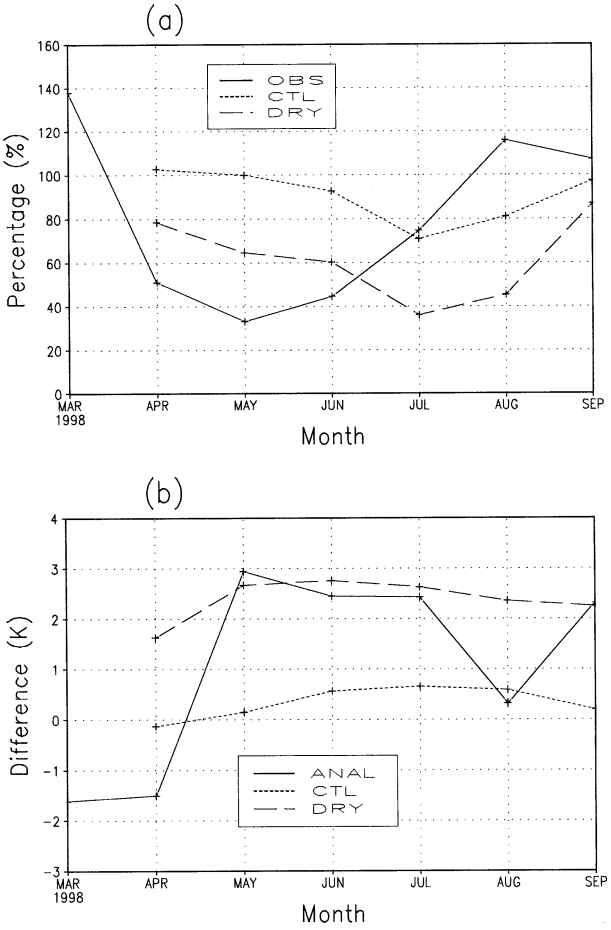

FIG. 15. (a) The percentage difference of domain-averaged precipitation for observation (solid line), and the control (dotted line) and dry (dashed line) experiments, and (b) for the corresponding temperature differences. Observational difference is obtained from the 1998 observed precipitation over the climatology during 1949–98, whereas the differences for the model simulation for the CTL and DRY experiments are computed over the simulation with climatological soil moisture (CLM). The difference of analyzed temperature (ANAL) is computed over the reanalysis climatology during 1949–98.

which is nearly the same as that from the RSM experiments. In August, the effect of the local soil moisture feedback weakens, and by September the precipitation is back near its climatological value. The surface temperature changes in a similar fashion, but weaker than observed (Fig. 15b). Reanalysis shows a dramatic increase of surface temperature as the drought is established. The temperature anomaly increases by 4.0 K during April–May. This heat anomaly persists throughout the drought, except for August when above-normal precipitation occurred in southern Texas. Weak heat anomalies during April and May from the CTL run indicate that the heat wave was established by SST anomalies with favorable atmospheric structure, as was the case for precipitation. Regional feedback due to subsequent dryness of soil moisture plays a role in maintaining the heat wave.

Since the RSM experiments were performed with reanalysis soil moisture only for the lowest soil model layer, it is possible that its positive feedback on the drought may have been underestimated. To test the effect of an intense deficit in the soil moisture, we also performed an experiment in which the lower soil model moisture was maintained at the wilting point. The results of the DRY experiment are also presented in Fig. 15. In this case the reduction of precipitation are much larger, and the increase in surface temperature is of the order of 2.5–3 K, both in agreement with observations. These results suggest that soil moisture feedback alone could maintain an extreme drought through local feedback. The fact that by September the precipitation recovers to near-normal levels even in the DRY experiment supports the conclusion that the end of the drought was associated with synoptic weather events not affected by local feedbacks.

From the above findings, we may can say that soil moisture anomalies have contributed to the maintenance

of the drought through a positive feedback due to deficit in local evaporation (Wolfson et al. 1987; Atlas et al. 1993; Koster et al. 2000). An additional impact of a high-albedo positive feedback (Charney 1975) which was not included in our experiments, may have also contributed to the observed drought. The drought ended in September–October and was followed by higher than normal precipitation (Fig. 2f). The same mechanism suggested by Atlas et al. (1993) for the demise of the heat wave and drought of 1988 was probably valid in 1998. In the fall, when solar radiation forcing (driving the regional reinforcing of the drought) became small, weather perturbations were able to penetrate the OK–TX region and break the persistent circulation pattern maintaining the drought.

The result of these experiments agree with our second hypothesis that once the drought pattern was established by SST anomalies during the spring and early summer, the reduction in local evaporation maintained the drought throughout the summer until early fall, even after the SST anomalies subsided. This hypothesis is also supported by the fact that during the summer of 1998, the operational 15-day ensemble forecasts maintained the drought with good agreement among forecasts. This also suggests that the anomalous soil moisture forcing was quite strong in maintaining the drought even in the 2-week global forecasts. Our results support the hypotheses described in section 3a, and that in Fig. 7.

6. Conclusions

From the global and regional model experiments for investigating the initiation and maintenance of the 1998 OK–TX drought, we found that the SST anomalies during April–May 1998, when the ENSO episode was starting to wane, established the conditions for the drought. However, the warm ENSO SST anomalies over the central and eastern tropical Pacific did not play as significant role in initiating the drought as the western Pacific anomalies and the cold anomalies in the Gulf of Mexico. In addition, the internal structure of atmospheric conditions (influenced by the SST anomalies in previous months) played as significant a role as the SST anomalies. The dry soil moisture anomalies established in spring resulted in a positive feedback to subsequent water deficit throughout the summer. Based on the experiments conducted in this study, we attempt to quantify the effect of SST and soil moisture anomalies, and the atmospheric internal forcing on the initiation and maintenance of the 1998 OK–TX drought. The impact of soil moisture anomalies should be focused on the RSM results, and the impact of SST anomalies in the global model framework. The difference of precipitation deficit in observation and simulated precipitation deficit can be attributed to the internal atmospheric forcing. The percentage change of precipitation over the OK–TX region resulting from various experiments is summarized in Table 2. The scenario proposed in this study qualitatively follows that in the Hong and Kalnay (2000), but is quantitatively different because we have included more ensemble members in the GCM simulations.

TABLE 2. Percentage change of monthly precipitation (%) over the OK–TX region due to the contribution of SST and SM anomalies estimated from the global (OSST−CSST) and regional (CTL−CLM) models, respectively. The reduction of observed precipitation (OBS) relative to the climatology during 1949–98 is also shown. A dash means that estimates from experiments are not available. Internal forcing for May 1998 represents the impact of the initial conditions for May 1998 (SMSST) vs the 1993 initial condition experiments (1993). Values in parentheses are estimates of internal forcing that would be required to explain the observed deficits.

	Apr	May	Jun	Jul	Aug	Sep
OBS	−48	−65	−55	−25	15	8
SST	−19	−35	−18	—	—	—
SM	2	0	−8	−30	−18	−2
Internal forcing	(−31)	−30	(−29)	—	—	—

In May 1998, SST anomalies explain a reduction of precipitation by 35%, which is smaller that the observation by about 30%. This 30% reduction can be attributed to the atmospheric internal forcing established at the end of April of 1998. The importance of the internal forcing expressed in the initial conditions is confirmed by the experiment with 1993 performed for May 1998. Likewise, in April the onset of drought was rooted in SST anomalies and internal forcing, but weaker impact due to SST anomalies than in May. Because of the above-normal precipitation during February and March precipitation, soil moisture anomalies during April and May increased slightly precipitation. In June, soil moisture anomalies started to play a positive feedback due to water deficit in April and May, but the impact of SST anomalies is still larger than that due to soil moisture anomalies. An 18% and 8% reduction of precipitation can be attributable to the SST and soil moisture anomalies. The rest of reduction can be attributable to the internal atmospheric forcing. With subsequent water deficit starting in April, soil moisture anomalies played an important role in maintaining the drought, and its impact explained most of water deficit in July. After July, regional feedback remained significant, but synoptic-scale disturbances produced above-normal precipitation near the Gulf of Mexico states, and thus, the impact of soil moisture anomalies is confined in Oklahoma and Texas. Hence, the drought in Oklahoma and northern Texas lasting until early October can be explained by the local feedback due to soil moisture anomalies established by preceding water deficit. Note that La Niña started in July and prevailed during the second half of 1998. A cold anomaly in the tropical Pacific, particularly, in western Pacific, might play a role in maintaining the drought. However, the spatial scale of the drought after August was small, which would not be explained by a remote control due to SST anomalies.

In the past, regional climate models have generally been used as a tool to provide regional details embedded

within a low-resolution global model (e.g., Hong and Leetmaa 2000; Giorgi et al. 1993). To be useful in this context, the global model has to have skill in predicting planetary and large-scale seasonal and interannual anomalies. Regional climate models have also been used as a ''magnifying glass'' for providing regional details in seasonal predictions in the framework of operational forecasts (Mo et al. 2000). On the other hand, the present study, Hong and Kalnay (2000), and Hong and Pan (2000), demonstrate another important application of regional climate models: the isolation and understanding of internal forcing mechanisms embedded within the evolving climate signal. The facts that the large-scale circulation is forced to remain realistic by the use of reanalysis boundary conditions, and that the regional model provides no feedback to the large scale, allow isolating the regional feedbacks, something very difficult to attain within the standard approach of global model integrations.

Acknowledgments. The authors want to express their gratitude to M. Richman, K. Crawford, J. Basara, and M. Masutani for helpful discussions. Acknowledgment is also made to NCEP for computer time used in this research. The comments of two anonymous reviewers improved the manuscript. This research was supported by the Climate Environment System Research Center sponsored by the SRC program of Korea Science and Engineering Foundation.

REFERENCES

Atlas, R., N. Wolfson, and J. Terry, 1993: The effect of SST and soil moisture anomalies on GLA model simulations of the 1988 U.S. summer drought. *J. Climate,* **6,** 2034–2048.

Barnston, A. G., A. Leetmaa, V. E. Kousky, R. E. Livezey, E. A. O'Lenic, H. van den Dool, A. J. Wagner, and D. A. Unger, 1999: NCEP forecasts of the El Niño of 1997–98 and its U.S. impacts. *Bull. Amer. Meteor. Soc.,* **80,** 1829–1852.

Basara, J. B., D. S. Arndt, H. L. Johnson, J. G. Brotzge, and K. C. Crawford, 1999: An analysis of the drought of 1998 using the Oklahoma Mesonet. *Eos, Trans. Amer. Geophys. Union,* **79,** 258.

Bell, G. D., M. S. Halpert, C. F. Ropelewski, V. E. Kousky, A. V. Douglas, R. C. Schnell, and M. E. Gelman, 1999: Climate assessment for 1998. *Bull. Amer. Meteor. Soc.,* **80,** S1–S48.

Caplan, P., J. Derber, W. Gemmill, S.-Y. Hong, H.-L. Pan, and D. Parrish, 1997: Changes to the 1995 NCEP operational medium-range forecast model analysis-forecast system. *Wea. Forecasting,* **12,** 581–594.

Charney, J. G., 1975: Dynamics of deserts and drought in the Sahel. *Quart. J. Roy. Meteor. Soc.,* **101,** 193–202.

Chen, P., and M. Newman, 1998: Rossby wave propagation and the rapid development of upper-level anomalous anticyclones during the 1988 U.S. drought. *J. Climate,* **11,** 2491–2504.

Fennessy, M. J., and J. Shukla, 1999: Impact of initial soil wetness on seasonal atmospheric prediction. *J. Climate,* **12,** 3167–3180.

Giorgi, F., M. R. Marinucci, and G. T. Bates, 1993: Development of a second-generation regional climate model (RegCM2). Part I: Boundary-layer and radiative transfer processes. *Mon. Wea. Rev.,* **121,** 2794–2813.

Hoffman, R. N., and E. Kalnay, 1983: Lagged-average forecasting, an alternative to Monte Carlo forecasting. *Tellus,* **35a,** 100–118.

Hong, S.-Y., 2000: Impact of the subgrid representation of parameterized convection on simulated climatology. NCEP Office Note 428, 32 pp.

——, and A. Leetmaa, 1999: An evaluation of the NCEP RSM for regional climate modeling. *J. Climate,* **12,** 592–609.

——, and E. Kalnay, 2000: Role of sea-surface temperature and soil-moisture feedback in the 1998 Oklahoma–Texas drought. *Nature,* **408,** 842–844.

——, and H.-L. Pan, 2000: Impact of soil moisture anomalies on seasonal, summertime circulation over North America in a regional climate model. *J. Geophys. Res.,* **105** (D24), 29 625–29 634.

——, H.-M. H. Juang, and D.-K. Lee, 1999: Evaluation of a regional spectral model for the East Asian monsoon case studies for July 1987 and 1988. *J. Meteor. Soc. Japan,* **77,** 553–572.

Juang, H. M. H., and S.-Y. Hong, 2001: Sensitivity of the NCEP regional spectral model to domain size and nesting strategy. *Mon. Wea. Rev.,* **129,** 2904–2922.

——, ——, and M. Kanamitsu, 1997: The NCEP regional spectral model. An update. *Bull. Amer. Meteor. Soc.,* **78,** 2125–2143.

Kalnay, E., and Coauthors, 1996: The NCEP/NCAR 40-Year Reanalysis Project. *Bull. Amer. Meteor. Soc.,* **77,** 437–471.

Koster, R. D., M. J. Suarez, and M. Heiser, 2000: Variance and predictability of precipitation at seasonal-to-interannual timescales. *J. Hydrometeor.,* **1,** 24–46.

Lyon, B., and R. M. Dole, 1995: A diagnostic comparison of the 1980 and 1988 U.S. summer heat wave-droughts. *J. Climate,* **8,** 1658–1675.

Mo, K. C., J. R. Zimmerman, E. Kalnay, and M. Kanamitsu, 1991: A GCM study of the 1988 United States drought. *Mon. Wea. Rev.,* **119,** 1512–1532.

——, M. Kanamitsu, H.-M. H. Juang, and S.-Y. Hong, 2000: Ensemble regional climate prediction for the 1997/1998 winter. *J. Geophys. Res.,* **105** (D24), 29 609–29 624.

Montroy, D. L., 1997: Linear relation of central and eastern North American precipitation to tropical Pacific sea surface temperature anomalies. *J. Climate,* **10,** 531–548.

——, M. B. Richman, and P. J. Lamb, 1998: Observed nonlinearties of monthly teleconnections between tropical Pacific sea surface temperature anomalies and central and eastern North American precipitation. *J. Climate,* **11,** 1812–1835.

Namias, J., 1991: Spring and summer 1988 drought over the contiguous United States—Causes and prediction. *J. Climate,* **4,** 54–65.

Palmer, T. N., and C. Brankovic, 1989: The 1988 United States drought linked to anomalous sea surface temperature. *Nature,* **338,** 54–57.

Reynolds, R. W., 1988: A real-time global sea surface temperature analysis. *J. Climate,* **1,** 75–86.

Seth, A., and F. Giorgi, 1998: The effect of domain choice on summer precipitation simulation and sensitivity in a regional climate model. *J. Climate,* **11,** 2698–2712.

Shukla, J., and Y. Mintz, 1982: The influence of land-surface evaporation on the earth's climate. *Science,* **215,** 1498–1501.

Takayabu, Y. N., T. Iguchi, M. Kachi, A. Shibata, and H. Kanzawa, 1999: Abrupt termination of the 1997–98 El Niño in response to a Madden–Julian oscillation. *Nature,* **402,** 279–282.

Ting, M., and H. Wang, 1997: Summertime U.S. precipitation variability and its relation to Pacific sea surface temperature. *J. Climate,* **10,** 1853–1873.

Trenberth, K. E., and G. W. Branstator, 1992: Issues in establishing causes of the 1988 drought over North America. *J. Climate,* **5,** 159–172.

——, ——, and P. A. Arkin, 1988: Origins of the 1988 North American drought. *Science,* **242,** 1640–1645.

Wang, W., and A. Kumar, 1998: A GCM assessment of atmospheric seasonal predictability associated with soil moisture anomalies over North America. *J. Geophys. Res.,* **103,** 28 637–28 646.

Wolfson, N., R. Atlas, and Y. C. Sud, 1987: Numerical experiments related to the 1980 heat wave. *Mon. Wea. Rev.,* **115,** 1345–1357.

Xie, P., and P. A. Arkin, 1996: Analyses of global monthly precipitation using gauge observations, satellite estimates, and numerical model predictions. *J. Climate,* **9,** 840–858.